Journal of Neurocytology **20**, 978–988 (1990)

Irregular geometries in normal unmyelinated axons: a 3D serial EM analysis

M. M. GREENBERG, C. LEITAO, J. TROGADIS and J. K. STEVENS*

Playfair Neuroscience Unit, Toronto Western Hospital, and University of Toronto, 399 Bathurst Street, Toronto Ontario, M5T 2S8, Canada

Received 16 January 1989; resubmitted 16 November 1989; revised 18 January 1990; accepted 1 February 1990

Summary

Axons have generally been represented as straight cylinders. It is not at all uncommon for anatomists to take single cross-sections of an axonal bundle, and from the axonal diameter compute expected conduction velocities. This assumes that each cross-section represents a slice through a perfect cylinder. We have examined the three-dimensional geometry of 98 central and peripheral unmyelinated axons, using computer-assisted serial electron microscopy. These reconstructions reveal that virtually all unmyelinated axons have highly irregular axial shapes consisting of periodic varicosities. The varicosities were, without exception, filled with membranous organelles frequently including mitochondria, and have obligatory volumes similar to that described in other neurites. The mitochondria make contact with microtubules, while the other membraneous organelles were frequently found free floating in the cytoplasm. We conclude that unmyelinated axons are fundamentally varicose structures created by the presence of organelles, and that an axon's calibre is dynamic in both space and time.

These irregular axonal geometries raise serious doubts about standard two dimensional morphometric analysis and suggest that electrical properties may be more heterogeneous than expected from single section data. These results also suggest that the total number of microtubules contained in an axon, rather than its single section diameter, may prove to be a more accurate predictor of properties such as conduction velocity. Finally, these results offer an explanation for a number of pathological changes that have been described in unmyelinated axons.

Introduction

Textbooks commonly teach that an unmyelinated axon's shape does not vary much over its length (cf. Berthold, 1978, p. 3; Carpenter & Sutin, 1983) and most research has assumed that unmyelinated axons are approximate cylinders. Consequently, single section measurements of diameter are typically taken whenever it is important to know the size of axons under study. Recent examples of this approach of relating axonal cross-sectional area or calibre to physiological or pathological properties are numerous (Fukada *et al.*, 1984; Gallego & Belmonte, 1984; Hsiao *et al.*, 1984; Scwab *et al.*, 1984; Smith & Rosenheimer, 1984; Cottrell & Hunter, 1985; Sanchez *et al.*, 1986; Woodbury & Ulinski, 1986). However, many early physiological studies report the breakdown of the square root law when relating conduction velocity to axonal diameter, particularly in small unmyelinated axons (Gasser, 1950, 1955; Paintal, 1966, 1967; see also Stein & Pearson, 1971).

To explain the discrepancy between axon diameter and conduction velocity, these earlier investigators concluded that smaller type C axons have different membrane properties. A second possibility not considered was that the small unmyelinated axons may not have homogeneous axial geometries. Non-cylindrical axonal geometries (with the exception of axonal terminations) such as swellings and varicosities, are most often associated with either pathology or fixation artifacts. However, much of our own work using serial electron microscopy (Ellias & Stevens, 1980; Sasaki *et al.*, 1983; Sasaki *et al.*, 1984; Jacobs & Stevens, 1986a, b; Stevens *et al.*, 1988) and time lapse photography (Jacobs & Stevens, 1986b, 1987) suggests that the axial calibre of most normal *in vivo* neurites is quite irregular. Moreover, one study using semi-serial sections (Aguayo *et al.*, 1976), also suggests that unmyelinated axons may be irregular.

If similar irregularities occur in unmyelinated axons

* To whom correspondence should be addressed.

0300–4864/90 $03.00 + .12

there are important implications. First, since axial geometry plays an important role in determining a neurite's space constant (Ellias & Stevens, 1980; Ellias *et al.*, 1985) longitudinal irregularities would introduce uncertainty about an axon's conduction velocity. Second, longitudinal irregularities would also introduce uncertainty into standard morphometrics used to predict an axon's conduction velocity. Finally, these geometric variations may also suggest unsuspected mechanisms of axonal function active both in normal and pathological axons, and might explain the earlier discrepancy between axonal diameter and conduction velocity.

The focus of this paper is therefore, to determine, via serial EM reconstruction, the full three-dimensional shape *in vivo* of normal unmyelinated axons. Specifically, we have examined unmyelinated axons from mouse sciatic nerve and cat retinal axons to see whether they have irregular longitudinal geometries similar to those we have seen in other neurites, or if they have cylindrical longitudinal shapes. Additionally, in an attempt to understand the cellular mechanisms that control axon shape we have quantitatively characterized the volumetric relationships between organelles, microtubules and plasma membrane.

Materials and methods

Electron microscopy

A variety of perfusion and immersion fixation protocols was tried on about 20 mouse (Balb/c young adult male) sciatic nerves. Perfusion was a poor choice in this case due to the small calibre of the blood vessels interspersed within the nerve bundle, leading to slow and inadequate penetration of the fixative. Thus, we used *in situ*, followed by immersion fixation. The sciatic nerve was surgically exposed. A pocket was created from the surrounding muscles, bathed continuously with fixative of 2.5% glutaraldehyde in microtubule-stabilizing buffer, 2[N-Morpholino]ethanesulfonic acid (MES), for 15 min. The perineurium surrounding the nerve was gently removed, the nerve transected, removed and dropped into fixative where it was further cut into 2 mm pieces. Total fixation time was 2 hours. The nerves were postfixed in osmium tetroxide, sequentially dehydrated in ethanol, immersed in propylene oxide, and embedded in Epon. The tissue blocks were serially cut into pale gold sections with a diamond knife on an ultramicrotome. The sections were then mounted onto formvar-coated grids and stained with uranyl acetate and lead citrate. The serial sections were photographed in a JEOL 100CX electron microscope, and the photomicrographs were analyzed by a computer-assisted serial EM reconstruction system (Stevens & Trogadis, 1984). This study used four such axons from four separate mice.

Cat retinae were collected after perfusion with glutaraldehyde using methods described by McGuire and co-workers (1986). All axons from the retina were sampled at a point before their entry into the optic disk.

In total, 79 unmyelinated sciatic axons and 19 ganglion cell axons were reconstructed. Sequential, uninterrupted serial sections from the 98 different axons were reconstructed into segments using series of 50–100 serial sections. Sciatic segments were each about 5 μm long, while retinal segments were about 8 μm. Volumes were computed for each serial slice of each axon assuming a 0.1 μm section thickness. We refer to these volumes as 'cross-sectional volumes'.

The reconstructed axons were not selected in any way. Entire Schwann cell units, or bundles of 10 or more unmyelinated sciatic axons enclosed by a single, continuous Schwann cell membrane similar to that seen in Fig. 1, were randomly chosen and every axon within the bundle was reconstructed. In the case of the ganglion cells, every complete axon in the EM field of the micrograph was reconstructed.

Computer reconstruction and display

Details of the computer-assisted serial reconstruction system may be found elsewhere (Stevens & Trogadis, 1984). All morphometrics and numerical analyses were computed using this system.

Solid body displays with microtubules, organelles and plasma membrane were produced using an ISG Technologies (Toronto, Ont.) ICAR 80.8 graphics workstation. All surfaces were computed using a Linear Surface Extrapolation (LSE) algorithm (Leitao *et al.*, 1988), developed specifically for display of biological objects. Microtubules were represented taking microtubule associated proteins, as well as actual microtubular diameter into account (see Fig. 5).

Quantitative analysis

Nine axons had individual organelles clearly isolated within a varicosity. These were analyzed in detail as described in previous publications (see Sasaki *et al.*, 1983, 1984; Jacobs & Stevens 1987b; Stevens *et al.*, 1988). The section-by-section volume for the axolemma, mitochondria, and smooth endoplasmic reticulum (SER) were plotted on a graph (Fig. 6). These plots all assume a section thickness of 0.1 μm. The microtubules (MT) were also plotted on this same graph assuming a base diameter of 24 nm plus 46 nm to allow for the microtubule associated proteins (MAPS) and a 23% packing allowance (Stevens *et al.*, 1988). A three sample sliding average was taken to remove local variation and a first order differential was taken. The total axolemma volume within the two minima and a single maximum of each varicosity was computed. This axonal volume and the total organelle volume for each of the nine axons was plotted on a separate graph (Fig. 8). A best-fit line was calculated using conventional least-squares methods.

Results

Inter-axonal differences

Axons within a single mouse Schwann cell unit have a wide variety of diameters (see Fig. 1). Mean cross-sectional volumes were computed for 79 sciatic axons. The mean was 0.0275 μm^3 (equivalent to a 0.6 μm diameter cylinder) with a range from 0.005 to 0.08 μm^3. The largest was 16 times the smallest. The 19 retinal ganglion cell axons had a slightly smaller mean of 0.0175 μm^3 (0.47 μm diameter cylinder).

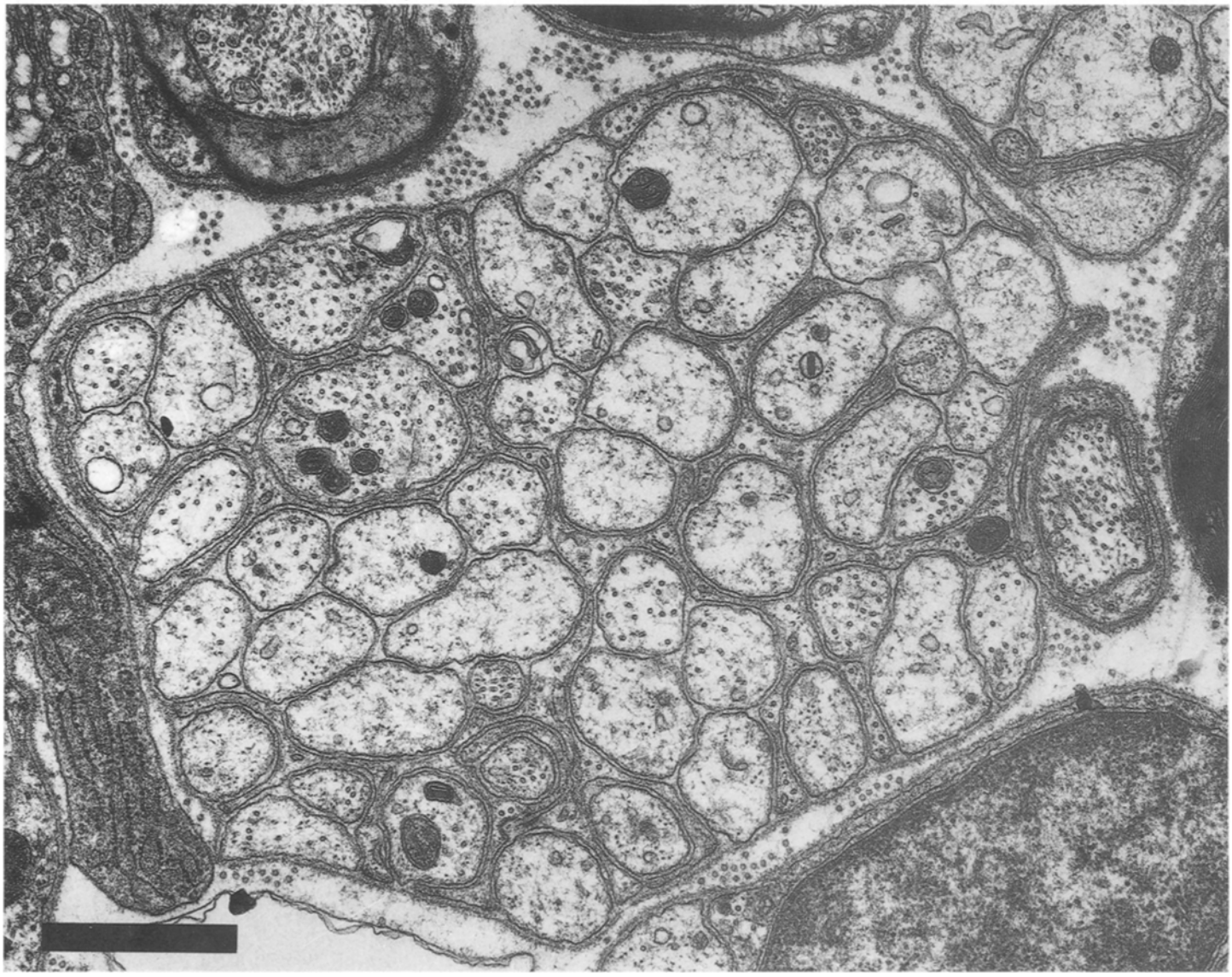

Fig. 1. A Schwann cell unit from a murine sciatic nerve surrounding a group of axons, and so identified because a single continuous Schwann cell basement membrane encloses a bundle of unmyelinated axons. Scale bar: 1 μm. Microtubules, mitochondria, axolemma and SER, are all evident in this micrograph.

Intra-axonal differences

Complete reconstructions of individual axons showed wide variation in cross-sectional volume over their lengths (Figs 2, 4 and 5). We quantified this variability using a simple ratio of an axon's maximum cross-sectional volume to its minimum cross-sectional volume. These values were obtained from reconstructions similar to those in Fig. 2. Figure 3 shows a histogram of 'max/min' ratios of 79 sciatic axons similar to those shown in Figs 1 and 2. No axon had a max/min ratio of unity, which would be expected for a cylinder. A max/min ratio of two is an axon with one region that is twice the cross-sectional area of another region of the same axon. The mode stands at 2.5, and the histogram shows that approximately 90% of the axons have max/min ratios of two or greater. Over one third of all the axons had varicose regions that were at least three times the volume of their necks, and over half of these varied in their cross-sectional volumes by a factor of at least four.

To provide a visual sense of the variation implied by these ratios, Fig. 4 shows reconstructions of four sciatic axons drawn beside their max/min ratios (1.5, 3, 6 and 10).

The 19 retinal ganglion cell axons had a distribution similar to that shown in Fig. 3.

When each axon's max/min ratio is plotted against its minimum cross-sectional volume (i.e. its neck), as shown in Fig. 9, a consistent pattern appears. The

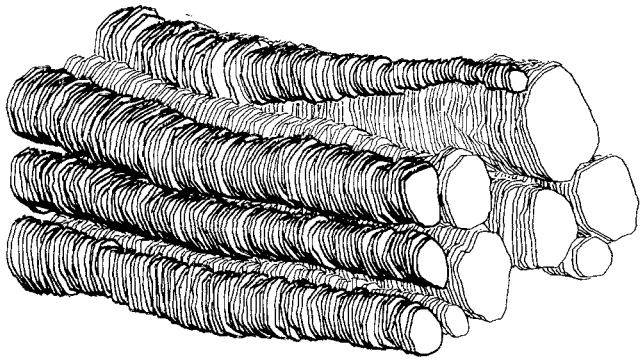

Fig. 2. A serial EM reconstruction of 11 axons from a Schwann cell unit similar to that shown in Fig. 1. It is clear that axons taken at any cross-section will be of many different sizes, and some axons undergo dramatic changes in calibre. The display includes perspective correction and absolute calibration bars are not possible. The small neck seen in the upper left has a diameter of 0.19 μm.

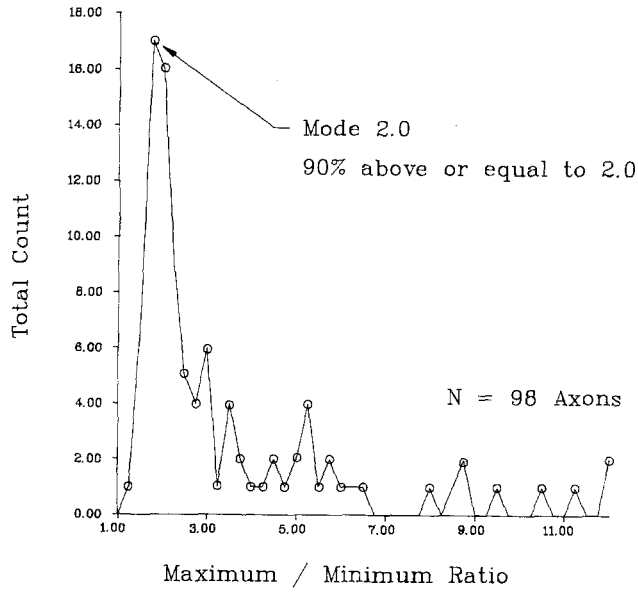

Fig. 3. Plot of maximum axonal diameter divided by the minimum diameter for 98 axons. Seventy-nine axons were from the sciatic material, the other 19 were from cat retina.

largest axons have the smallest variation, while the *smallest* axons have the greatest variation. In general the data describe an asymptotic curve.

Contents of varicosities and necks

All the reconstructed expansions or varicosities enclose large membranous organelles and a few microtubules, while all necks contain cytoskeletal elements, such as microtubules and neurofilaments with the occasional smaller SER or dense body. The larger varicosities contain one (Fig. 5) or two (Fig. 7) mitochondria, but SER, smooth vesicular bodies, and dense bodies are also present. We include these three latter components in the 'SER' category in our displays and analysis. No mitochondrion was ever found that did not have a varicosity around it. The reconstructions seen in Figs 5 and 7 illustrate this fact and show microtubules, the outer plasma membrane, and the contained organelles.

Quantitative analysis was carried out on reconstructed axons similar to that shown in Figs 5 and 7. Figure 6 is a plot of the section-by-section volume of the axolemma, mitochondria and SER seen in Fig. 5. The total volume of the axolemma and contained organelles was computed from these data (see Methods) for nine axons. These data were plotted on a scatter graph and best fit was computed (Fig. 8). We found that the extra volume beyond the mitochondrial component, or what we have previously called the 'obligatory organelle volume' (see Sasaki *et al.*, 1983, 1984) was a linear function of the organelle volume. (Figs 6, 8),. These axons had an obligatory volume constant of 3.52 (slope of best-fit line in Fig. 8), with an $r = 0.97$. These results are consistent with previous non-axonal material (see Stevens *et al.*, 1988).

In addition, the number of axonal microtubules predicts the minimum neck volume. Based on measurements from previous work (Jacobs & Stevens, 1986a), if we assume each MT has a diameter of 24 nm and further assume that the MAPS add an additional 23 nm, a net exclusion diameter of 70 nm is created. Finally, a packing constant of 23% (see Jacobs & Stevens, 1986b; Stevens *et al.*, 1988) must be added. Again, this relationship may be seen in Figs 5 and 6, and is consistent with all other neuritic systems we have studied (Stevens *et al.*, 1988).

Thus, these axons have an internal organization similar to that described for cat retinal dendrites, and virtually identical to that described for PC12 neurites (Jacobs & Stevens, 1986a, b; Stevens *et al.*, 1988).

Organelle, microtubule and plasma membrane associations

One very interesting observation was that mitochondria often appear to make contact with groups or baskets of microtubules (Figs 5 and 7; Greenberg & Stevens, 1986). In contrast, the SER was most often found floating free in the cytoplasm making no contact with microtubules at all. These results are consistent with recent work of Cheng & Reese (1988) in chick optic tectum.

The plasma membrane associated with the varicosities was often highly asymmetric along the length of the axis. Varicosities had what could be described as a head and a tail with asymmetric slopes. In four of the nine axons the mitochondria 'led' the peak volume of

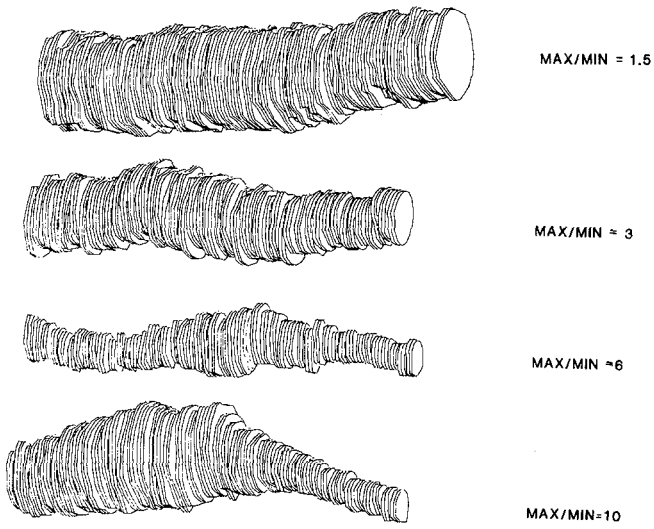

Fig. 4. Reconstructions from the same group shown in Fig. 2, showing visual appearance of an axon with different maximum/minimum ratios.

the plasma membrane by several tenths of a micrometer (see 'lag' in Fig. 6). These observations are what might be expected if an organelle were moving along the MTs. Unfortunately, we do not have independent verification of proximal and distal ends of the axons in this study. However, both of these results are now being confirmed quantitatively in larger sets of data with identified proximal and distal ends using cross-correlation and convolutions.

Discussion

Our data taken from central and peripheral axons suggest that many unmyelinated axons are varicose. The expanded portions of the axon range from 1.25 to 12 times the cross-sectional areas of the necks of the same axon. Moreover, since all varicosities contain membranous organelles the data also suggest that the varicosities are created by organelles.

The possibility that these expansions are due to fixation is unlikely for several reasons. First, we have used several different fixation methods (see Methods) with consistent results. When we reconstruct a complete group of adjacent axons in this material we see no evidence of poor fixation penetration or regional correlations or artifacts. Second, we see varicosities at the light level in living tissue culture cells similar to those seen in these axons. When this material is fixed using methods identical to those reported here, we see no change in cell shape at the light level (Jacobs & Stevens, 1986a, b, 1987). In contrast, when we intentionally depolymerize MTs using drugs such as Nocodazole, we see clear changes in neurite shape at the light level (Jacobs & Stevens, 1986b). Thus, any MT depolymerization due to fixation would lead to a detectable change in shape. Third, when this same tissue culture material is reconstructed at the EM level, organelles with an added obligatory volume similar to that seen in Figs 5–8 are found (Jacobs & Stevens, 1986a) in each varicosity. Microtubule starts and stops, presence of baskets and an organization similar to that seen in Figs 5 and 7 are also present. Finally, these results are consistent with independent physiological data, in that they explain the discrepancy between measured axonal diameter and conduction velocity (see below).

These data corroborate previous studies of dendrites and data from PC12 neurites (Sasaki *et al.*, 1983, 1984; Jacobs & Stevens, 1986a, b; Stevens *et al.*, 1988). These studies all concluded that a neurite's volume is composed of a baseline volume (equal to its neck) dependent on microtubules. To this baseline volume the mitochondria and other membranous organelles, along with their obligatory volumes, may be added to create the varicosity. These have the effect of modulating local volumes or cross-sectional areas depending upon the distribution of organelles, with the minimum volume determined by the total number of microtubules.

Much recent and classical work has shown that many membranous organelles move down along the axon (see Lasek & Brady, 1983; Martz *et al.*, 1984; Allen *et al.*, 1985; Vale *et al.*, 1985; Forman *et al.*, 1987). This implies that varicosities, which are associated with these organelles, must also move down along the axon. This conclusion is further supported by Koenig and colleagues (1985) who observed translation of varicosities in regenerating axons as well as our own light level, time lapse observations in PC12 cells (Jacobs & Stevens, 1987). The lag between the mitochondria and axolemma seen in Fig. 6 also suggests active movement.

Consequently, an axon may be considered to have both temporal and spatial variation in calibre at any one point in its length.

Historical perspective

Neuritic varicosity is a concept more forgotten than new. It was first reported in 1893 along branches of

Fig. 5. Complete solid body reconstruction of an axon with all contained organelles and microtubules. Taken from a series of 48 serial sections. Each varicosity or expansion seen in all reconstructions contained organelles. The necks, or small diameter portions of an axon, contain mostly microtubules. The top figure shows the outer plasma membrane, and the lower figure shows the contained mitochondria (gold), SER (red) and microtubules (black). The neck is 0.23 μm in diameter.

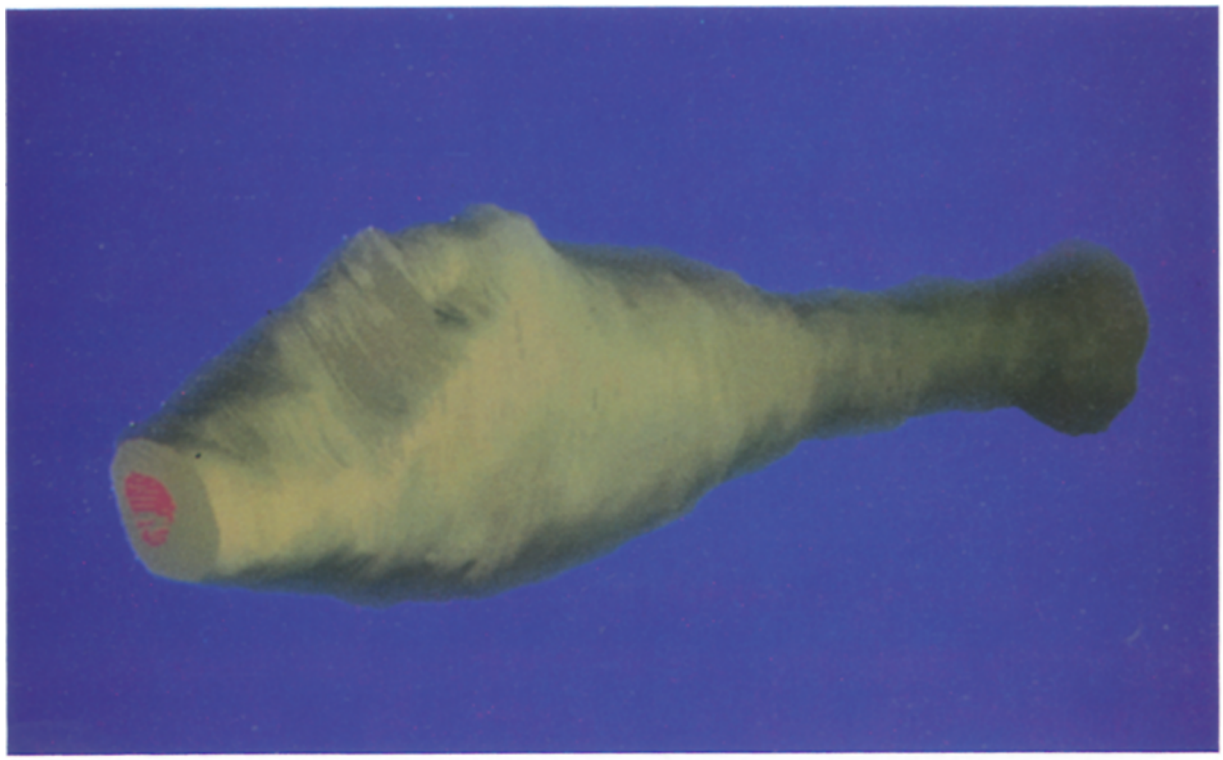

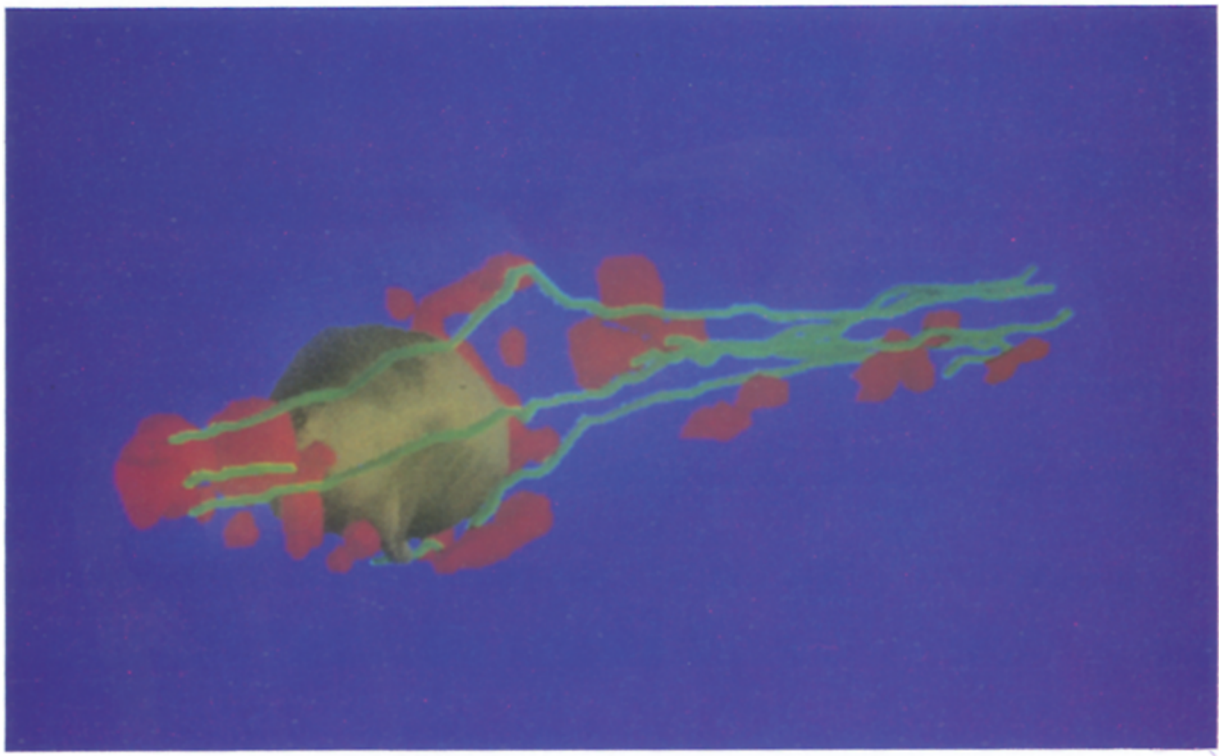

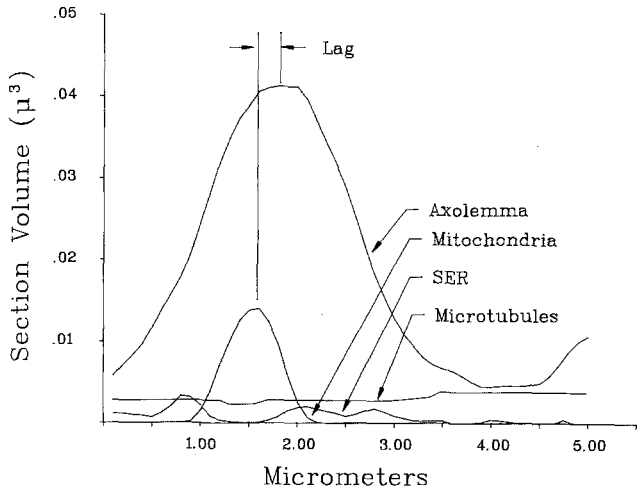

Fig. 6. Plot of axolemma, organelle and MT cross-sectional volume as a function of section number for the reconstruction seen in Fig. 5. The axolemma, SER, mitochondrial, and microtubular volume are all labelled. The 'lag' shown above represents the displacement between the peaks of the axolemma volume and the mitochondrial volume.

pyramidal processes prepared by the Golgi method (see Black, 1981). Many other reports of varicosities followed, based on both experimental and clinical staining techniques. There arose a great debate over their presence and functional meaning. However, in 1899 Weil & Frank published a short preliminary report of a three-year study which demonstrated that varicosities were artifacts of the Golgi method. The full report was never published. Though the conclusion was never substantiated, their preliminary data nevertheless seems historically to have closed the debate over varicosities, and many continue to believe they are artifacts (reviewed in Black, 1981).

Varicosities in normal and pathological preparations

Varicosities have most commonly been associated with pathology. For example, they have been reported in neuroaxonal dystrophy (Coers & Woolf, 1959; Seitelberger, 1971; Jellinger & Jirasek, 1971), in degenerating and regenerating sciatic axons of rats (Morris *et al.*, 1972; Koenig *et al.*, 1985), in ligated axons (Griffin *et al.*, 1977), in CNS disorders (Suzuki & Zagoren, 1975), and in toxic neuropathies (Chou & Hartmann, 1964; Koenig, 1969).

Only a limited number of examples of varicosities have been reported in normal material. Adrenergic terminals all have varicosities, usually filled with synaptic vesicles and dense core granules (mouse vas deferens axons: Basbaum & Heuser, 1979; guinea pig myenteric plexus: Jonakait *et al.*, 1979; bovine splenic nerve: Thureson-Klein *et al.*, 1979; rat superior cervical ganglion, dissociated and cultured: Buckley & Landis, 1983). Varicosities have not been generally recognized in normal axons proximal to synaptic terminals. Ochs & Jersild (1987) reported beading of axons that were stretched and then processed by freeze-substitution. These beadings constituted constrictions of 10–25 μm in length with a period of 20–50 μm. Leonhardt (1976) reported 'axonal spheroids', or swellings, in the spinal cords of normal rabbits. Most of these myelinated and unmyelinated spheroids were packed with mitochondria, dense bodies, vesicles, and fragments of SER. Leonhardt suggested that these swellings reflect aging, not disease, a conclusion disputed by Clark and colleagues (1984), who suggested that they play a role in remodelling the CNS.

Aguayo and colleagues (1976) performed a 'semi-serial' EM study of unmyelinated fibres in the rat cervical sympathetic trunk but reported no varicosities. However, the main interest of the Aguayo paper was in axon-Schwann relationships and the question of varicosities was not directly addressed. They sampled every 20th section from the mid-level of each trunk, and performed EM upon these to follow individual axons through a length of about 120 μm. The interval between two successive thin sections was 2–6. Thus, it would be impossible for them to detect varicose expansions such as we report here of about 2 to 6 μm in length. Although not critical to their central conclusions, these data also show that it would be very difficult to identify the same axon from one section to the next with samples of 2–6 μm.

Ellias & Stevens (1980) and Sasaki and co-workers (1983, 1984) reported varicosities in retinal amacrine cells that were later confirmed by Famiglietti (1985). Jacobs & Stevens (1986b) examined cultured PC12 neurites by serial EM, and found that varicosities were common at all developmental stages. Moreover, these workers were able to observe varicosities at the light level in living PC12 tissue culture cells moving along the neurite length (Jacobs & Stevens, 1987).

Uncertainty and single-section analysis

The presence of axonal varicosities raises serious practical morphometric problems. Any single static measurement of axonal diameter will fail to reflect a spatially changing axon. Our studies show that small axons are more irregular than larger ones. This leads to the following predicament for conventional EM in measuring the cross-section of an axon on one or a few sections. Figure 9 shows that the smaller the cross-sectional area, the greater the likelihood that the axon expands elsewhere (or expands later in the same place). By the same token, a large axonal cross-section may either belong to a large and nearly cylindrical axon or to a small but varicose axon. Consequently, conventional EM cannot be used to measure axonal size with any confidence.

Figure 10 compares the results of conventional two-dimensional cross-sectional analysis with serial

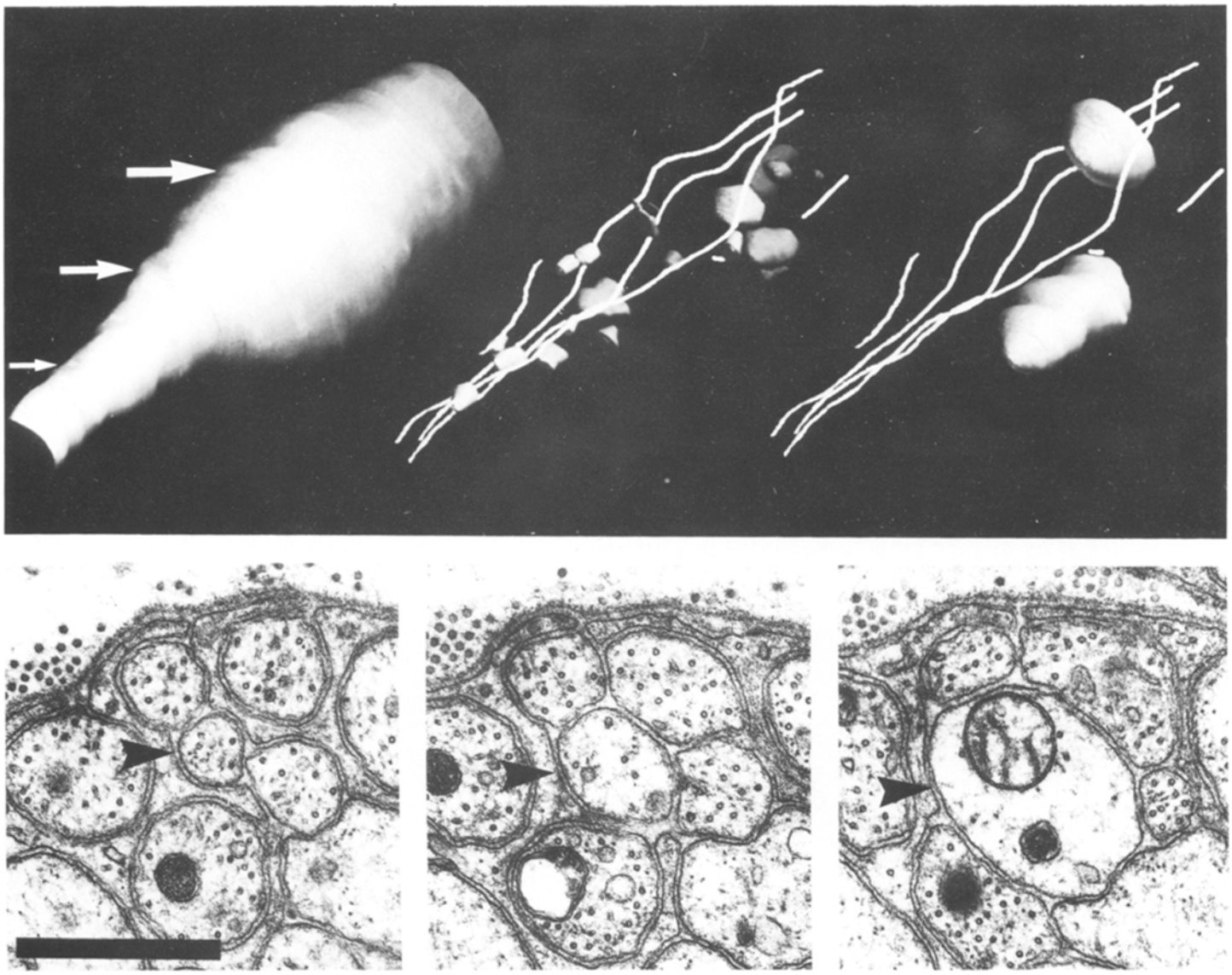

Fig. 7. (A) Solid body reconstruction of varicose axon (left) from 48 continuous serial sections with microtubules and SER (middle), microtubules and mitochondria (right). Arrows on left side indicate the levels of the sample micrographs shown in in (B). (B) Selected electron micrographs from series of 48 sections sampled at arrows seen in (A). Micrograph on left side is section number 4, middle micrograph is section number 14, and far right micrograph is section number 35. Scale bar: 1 μm.

EM analysis of the same 79 axons. Random samples of diameters were taken within the series and plotted as single random sample diameters on the abscissa. The actual maximum and minimum diameters from the same axon taken from the serial sections were plotted on the ordinate. If the axon were a straight cylinder then its maximum and minimum as well as a randomly taken diameter would have identical values. This perfect cylinder is represented by the straight line ($y = x$) in the figure. The standard deviation from this straight line value is $\pm 0.145\,\mu m$ and a 0.51 best fit r squared.

The envelope enclosing the points is the actual range within which a single sampled diameter may fall in conventional EM. The extent to which this sample can be unrepresentative of its axon reflects the uncertainty associated with conventional morphometrics. This envelope of uncertainty is wider at the smaller sample volumes, and narrower at the larger sample volumes. This problem becomes most critical in attempts to relate physiological to morphometric data.

Functional implications

Early physiological studies report the breakdown of the square root law when relating velocity to axonal

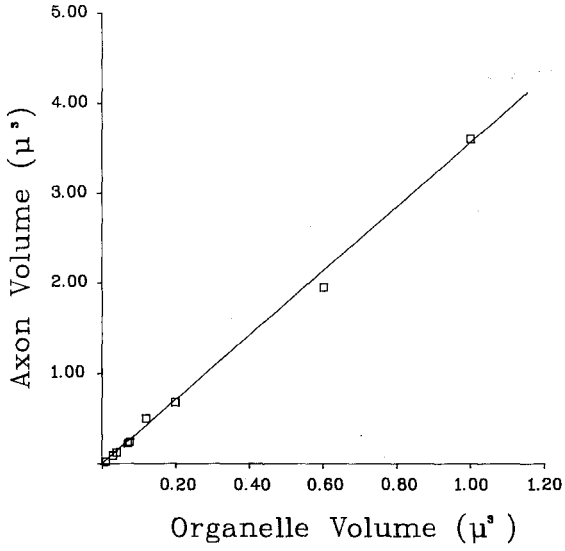

Fig. 8. Plot of total organelle volume vs the axonal plasma volume for nine axons. Graphs similar to that shown in Fig. 6 were created for each of the nine axons, and the two coordinates were computed by adding up all cross-sectional volumes over the range of the varicosity plotted (see Methods). The slope of the line is 3.52 with a straight line fit shown above having an r value of 0.97. The equation for the line is $V_A = V_O \times 3.52 - 0.016$.

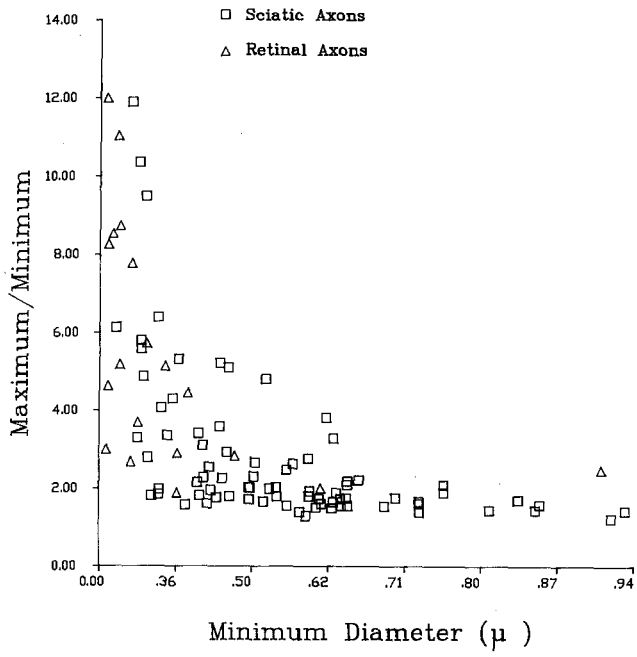

Fig. 9. Plot of each axon's max/min ratio against the minimal cross-sectional diameter of the axon's neck, ie. against its narrowest (baseline) cross-section. Axons with the smallest diameter necks also have the largest varicosities.

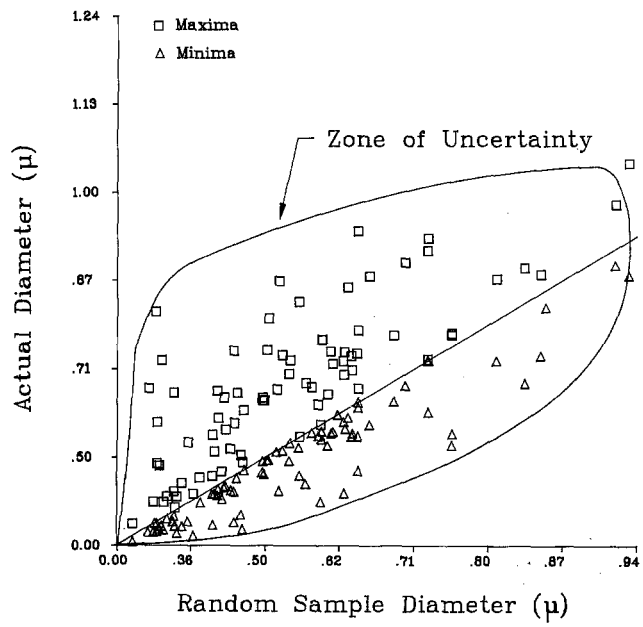

Fig. 10. Plot of results of conventional EM against serial EM, showing 79 single EM samples taken randomly from our material with actual maximum and minimum values. Random diameter samples were taken from the original electron micrographic prints. The axon was identified and reconstructed. The actual maximum section diameter was plotted using a square symbol and the actual minimum diameter was plotted as a triangle. The case of the straight cylinder is represented by a line. An envelope or 'zone of uncertainty' encloses actual serial measurements of the maximal and minimal cross-sectional areas of each of the 79 axons. The standard deviation from this straight line value is ±0.145 μm and 0.51 is the r^2 best-fit line.

diameter in small unmyelinated axons (Gasser, 1950, 1955; Paintal, 1966, 1967; Stein & Pearson, 1971), an issue which received little subsequent attention. These earlier investigators concluded that smaller axons must have different membrane properties. The presence of axonal varicosities, without special membrane properties may be a more parsimonious explanation of their observations.

Ellias & Stevens (1980) and Ellias and co-workers (1985) have shown that in almost all cases a neural process which has a volume redistribution that departs in any way from a cylinder will have a space constant below even the smallest equivalent cylinder. Based on that data these axonal varicosities will always decrease conduction velocity below that predicted for any single cross-section sample at any point along the length of the axon. In other words, the only time axonal diameter can ever be used to accurately predict conduction velocity will be when the axon is a perfect cylinder. Otherwise, in almost all cases, the conduction velocity will be slower than that predicted for *even the actual minimum diameter* of the reconstructed axon

(Ellias *et al.*, 1985). This compounds the conduction velocity error far beyond that suggested even by Fig. 9.

The major interesting result from this study is the relationship between axon shape and mitochondria, SER and microtubules. The maximum axonal diameter is determined by the organelles and their obligatory volume. The minimum axonal diameter is determined by the total number of microtubules. For example, the micrographs seen in Fig 7b (right image) show a large diameter neurite with only a few MTs. This may initially appear *abnormal*, but in the same neurite only 30 sections away we see a much smaller calibre neck with the same number of MTs that appears quite *normal*. It is important to emphasize that depending upon the distribution of organelles and MTs along the length of a neurite these maximums and minimums may or may not actually be achieved. Nevertheless, we can safely conclude that a large axon with only a few MTs will be varicose and will likely have a much smaller neck someplace along its length. This in turn could have a dramatic impact on axonal conduction velocity.

We have previously reported that if varicosities are spaced greater than their own diameter apart the neurite will always have a space constant near or below the minimum neurite diameter (Ellias & Stevens, 1980; Ellias *et al.*, 1985). Thus, one interesting possibility is that the total number of microtubules seen on any axonal cross-section (small or large diameter) may actually be a better predictor of axonal conduction velocity than diameter or size of the axon.

Acknowledgements

This work was supported by a grant from the Kroc foundation, and the Canadian Medical Research Council. We thank ISG Technologies for the ICAR 80.8 workstation, to produce Figs 5 and 7.

References

AGUAYO, A. J., BRAY, G. M., TERRY, L. C. & SWEEZEY, E. (1976) Three dimensional analysis of unmyelinated fibers in normal and pathologic autonomic nerves. *Journal of Neuropathology and Experimental Neurology* **35**, 136–51.

ALLEN, R. D., WEISS, D. G., HAYDEN, J. H., BROWN, D. T., FUJIWAKE, H. & SIMPSON, M. (1985) Gliding movement and bidirectional transport along single native microtubules from squid axoplasm: evidence for an active role of microtubules in cytoplasmic transport. *Journal of Cell Biology* **100**, 1736–52.

BASBAUM, C. B. & HEUSER, J. E. (1979) Morphological studies of stimulated adrenergic axon varicosities in the mouse vas deferens. *Journal of Cell Biology* **80**, 310–25.

BERTHOLD, C.-H. (1978) Morphology of normal peripheral axons. In: *Physiology and Pathobiology of Axons* (edited by WAXMAN, S. G.) New York: Raven Press.

BLACK, S. E. (1981) Pseudopods and synapses: the amoeboid theories of neuronal mobility and the early formulation of the synapse concept, 1894–1900. The Osler Medical Essay. *Bulletin of the History of Medicine* **55**, 34–58.

BUCKLEY, K. M. & LANDIS, S. C. (1983) Morphological studies of synapses and varicosities in dissociated cell cultures of sympathetic neurons. *Journal of Neurocytology* **12**, 67–92.

CARPENTER, M. B. & SUTIN, J. (1983) *Human Neuroanatomy*. Baltimore: Williams and Wilkins.

CHENG, T. P. & REESE, T. S. (1988) Compartmentalization of anterogradely and retrogradely transported organelles in axons and growth cones from chick optic tectum. *Journal of Neuroscience* **8**, 3190–9.

CHOU, S. M. & HARTMANN, H. A. (1964) Axonal lesions and waltzing syndrome after IDPN administration in rats. With a concept- 'axostasis'. *Acta Neuropathologica* **3**, 428–50.

CLARK, A. W., PARHAD, I. M., GRIFFIN, J. W. & PRICE, D. L. (1984) Neurofilamentous axonal swellings as a normal finding in spinal anterior horn of man and other primates. *Journal of Neuropathology and Experimental Neurology* **43**, 253–62.

COERS, C. & WOOLF, A. L. (1959) *The Innervation of Muscle*. Oxford: Oxford University Press.

COTTRELL, D. F. & HUNTER, J. M. (1984) Scaling factor relating conduction velocity and transverse axon profile for nonmyelinated alimentary nerves. *Experimental Neurology* **90**, 700–2.

ELLIAS, S. A. & STEVENS, J. K. (1980) The dendritic varicosity: a mechanism for electrically isolating the dendrites of cat retinal amacrine cells? *Brain Research* **196**, 365–72.

ELLIAS, S., GREENBERG, M. & STEVENS, J. K. (1985) Active and passive propagation in inhomogeneous axons: theoretical and serial EM studies of varicose unmyelinated nerves. *Society for Neuroscience Abstracts*

FAMIGLIETTI, E. V. (1985) Starburst amacrine cells: morphological constancy and systematic variation in the anisotropic field of rabbit retinal neurons *Journal of Neuroscience* **5**, 562–77.

FORMAN, D. S., LYNCH, K. J. & SMITH, R. S. (1987) Organelle dynamics in lobster axons: anterograde, retrograde and stationary mitochondria. *Brain Research* **412**, 96–106.

FUKADA, Y., HSIAO, C. F., WATANABE, M. & ITO, H. (1984) Morphological correlates of physiologically identified Y-, X-, and W-cells in cat retina. *Journal of Neurophysiology* **52**, 999–1013.

GALLEGO, R. & BELMONTE, C. (1984) Axonal conduction velocity and input conductance in petrosal ganglion primary sensory neurons of the cat. *Neuroscience Letters* **52**, 117–22.

GASSER, H. S. (1950) Unmedullated fibers originating in dorsal root ganglia. *Journal of General Physiology* **33**, 651–90.

GASSER, H. S. (1955) Properties of dorsal root unmedullated fibers on the two sides of the ganglion *Journal of General Physiology* **38**, 709–28.

GREENBERG, M. M. & STEVENS, J. K. (1986) Organelles

organize microtubules into transient baskets: a serial EM 3D reconstruction of systems of axonal microtubules. *Society for Neuroscience Abstracts* **12**, 000–000.

GRIFFIN, J. W., PRICE, D. L., ENGEL, W. K. & DRACHMAN, D. B. (1977) The pathogenesis of reactive axonal swellings: role of axonal transport. *Journal of Neuropathology and Experimental Neurology* **36**, 214–27.

HSIAO, C. F., WATANABE, M. & FUKADA, Y. (1984) The relation between axon diameter and axonal conduction velocity of Y, X, and W cells in the cat retina. *Brain Research* **309**, 357–61.

JACOBS, J. R. & STEVENS, J. K. (1986a) Changes in the organization of the neuritic cytoskeleton during nerve growth factor-activated differentiation of PC12 cells: a serial electron microscopic study of the development and control of neurite shape. *Journal of Cell Biology* **103**, 895–906.

JACOBS, J. R. & STEVENS, J. K. (1986b) Experimental modification of PC12 neurite shape with the microtubule-depolymerizing drug Nocodazole: a serial electron microscopic study of neurite shape control. *Journal of Cell Biology* **103**, 907–15.

JACOBS, R. & STEVENS, J. (1987) Dynamics of behavior during neuronal morphogenesis in culture. *Cell Motility and the Cytoskeleton* **8**, 250–60.

JELLINGER, K. & JIRASEK, A. (1971) Neuroaxonal dystrophy in man: character and natural history. *Acta neuropathologica* **Suppl V**: 3–16.

JONAKAIT, G. M., GINTZLER, A. R. & GERSHON, M. D. (1979) Isolation of axonal varicosities (autonomic synaptosomes) from the enteric nervous system. *Journal of Neurochemistry* **32**, 1387–1400.

KOENIG, H. (1969) Acute axonal dystrophy caused by fluorocitrate: the role of mitochondrial swelling. *Science* **164**, 310–12.

KOENIG, E., KINSMAN, S., REPASKY, E. & SULTZ, L. (1985) Rapid mobility of motile varicosities and inclusions containing a-spectrin, actin, and calmodulin in regenerating axons in vitro. *Journal of Neuroscience* **5**, 715–29.

LASEK, R. J. & BRADY, S. T. (1983) Orthograde and retrograde particle movement in isolated axoplasm from the giant axon of the squid. *Journal of Cell Biology* **97**, A4.

LEITAO, C., STEVENS, J. & DEKEL, D. (1988) A rapid automatic algorithm for placing smooth three dimensional surfaces on complex contoured, biological objects. U.S. Patent application 1988.

LEONHARDT, H. (1976) 'Axonal spheroids' in the spinal cord of normal rabbits. *Cell & Tissue Research* **174**, 99–108.

MARTZ, D., LASEK, R. J., BRADY, S. T. & ALLEN, R. D. (1984) Mitochondrial motility in axons: membranous organelles may interact with the force generating system through multiple surface binding sites. *Cell Motility* **4**, 77–154.

McGUIRE, B. A., STEVENS, J. K. & STERLING, P. (1986) Microcircuitry of Beta ganglion cells in cat retina. *Journal of Neuroscience* **6**, 907–18.

MORRIS, J. H., HUDSON, A. R. & WEDDELL, G. (1972) A study of degeneration and regeneration in the divided rat sciatic nerve based on electron microscopy. III. Changes in the axons of the proximal stump. *Zeitschrift für Zellforschung* **124**, 131–64.

OCHS, S. & JERSILD, J. (1987) Cytoskeletal organelles and myelin structure of beaded nerve fibers. *Neuroscience* **22**, 1041–56.

PAINTAL, A. S. (1966) The influence of diameter of medullated nerve fibres of cats on the rising and falling phases of the spike and its recovery. *Journal of Physiology* **184**, 791–811.

PAINTAL, A. S. (1967) A comparison of the nerve impulses of mammalian non-medullated nerve fibres with those of the smallest diameter medullated fibres. *Journal of Physiology* **193**, 523–33.

SANCHEZ, R. M. & DUNKELBERGER, G. R., QUIGLEY, H. A. (1986) The number and diameter distribution of axons in the monkey optic nerve. *Investigative Ophthalmology and Visual Science* **27**, 1342–50.

SASAKI, S. STEVENS, J. K. & BODICK, N. (1983) Serial reconstruction of microtubular arrays in dendrites: the cytoskeleton of the vertebrate dendrite. *Brain Research* **259**, 193–206.

SASAKI-SHERRINGTON, S. E., JACOBS, J. R. & STEVENS, J. K. (1984) Intracellular control of axial shape in non-uniform neurites: a serial electron microscopic analysis of organelles and microtubules in AI and AII retinal amacrine neurites. *Journal of Cell Biology* **98**, 1279–90.

SCWAB, B. W., AREZZO, J. C., PALDINO, A. M., FLOHE, L., MATTHIESSON, T. & SPENCER, P. S. (1984) Rabbit sural nerve responses to chronic treatment with thalidomide and supidimide. *Muscle & Nerve* **7**, 362–8.

SEITELBERGER, F. (1971) Neuropathological conditions related to neuroaxonal dystrophy. *Acta Neuropathologica* **Suppl V**, 17–29.

SMITH, D. O. & ROSENHEIMER, J. L. (1984) Factors governing speed of action potential conduction and neuromuscular transmission in aged rats. *Experimental Neurology* **83**, 358–66.

STEIN, R. B. & PEARSON, K. G. (1971) Predicted amplitude and form of action potentials recorded from unmyelinated nerve fibres. *Journal of Theoretical Biology* **32**, 539–58.

STEVENS, J. K. & TROGADIS, J. (1984) Computer-assisted reconstruction from serial electron micrographs: a tool for the systematic study of neuronal form and function. *Advances in Cellular Neurobiology* **5**, 341–69.

STEVENS, J. K., TROGADIS, J. & JACOBS, R. (1988) Development and control of axial neurite form: A serial electron microscopic analysis. In *Intrinsic Determinants of Neuronal Form and Function* (edited by LASEK, R. & BLACK, M.) pp. 115–45. New York: Alan R. Liss.

SUZUKI, K. & ZAGOREN, J. C. (1975) Focal axonal swelling in cerebellum of Quaking mouse: light and electron microscopic studies. *Brain Research* **85**, 38–43.

THURESON-KLEIN, A., KLEIN, R. L. & JOHANNSSON, O. (1979) Catecholamine-rich cells and varicosities in bovine splenic nerve, vesicle contents and evidence for exocytosis. *Journal of Neurobiology* **10**, 309–24.

VALE, R. D., SCHNAPP, B. J., REESE, T. S. & SHEETZ, M. P. (1985) Movement of organelles along filaments dissociated from the axoplasm of the squid giant axon. *Cell* **40**, 449–54.

WOODBURY, P. B. & ULINSKI, P. S. (1986) Conduction velocity, size and distribution of optic nerve axons in the turtle, *Pseudemys scripta elegans*. *Anatomy of Embryology* **174**, 253–63.